NOISE-CON 2026
JULY 9–11 • LONG BEACH, CA
GOOD VIBRATIONS

Mitigating Grazing Flow Impedance Eduction Errors in Additively Manufactured Porous Liners

Kara Hardy[1], Anthony Ciletti [2], Janith Godakawela [3], Bhisham Sharma [4]
Mechanical and Aerospace Engineering, Michigan Technological University
Houghton, MI, United States

Martha Brown[5]
Flight Vehicle Acoustics Branch, NASA Langley Research Center
Hampton, VA, United States

ABSTRACT

Additively manufactured porous metamaterials, including triply periodic minimal surface (TPMS) cores, are promising candidates for aeroengine liners but often behave as extended-reacting treatments under grazing flow. Standard impedance eduction procedures assume locally-reacting behavior and can yield physically inconsistent results for such materials. This study evaluates internal partitions (thin solid walls inserted at regular intervals along the liner's streamwise extent) as a means of suppressing internal streamwise propagation to improve eduction consistency. Six TPMS configurations were tested in the NASA Langley Grazing Flow Impedance Tube (GFIT) at partition spacings of 4″, 2″, and 1″, as well as unpartitioned, and at Mach numbers up to 0.3. For most geometries, 2″ partition spacing eliminated impedance discontinuities and substantially improved Prony correlation, though effectiveness varied with core topology. Partitions also altered the acoustic response of the liners: resistance increased, resonance frequencies shifted downward, and peak attenuation decreased while bandwidth broadened in some cases. Because partitions modify the liner itself, the educed impedance characterizes the partitioned system rather than the original unpartitioned core. These results establish partitioning as a practical pathway toward liners that are more compatible with standard eduction methods, while demonstrating that the intervention is itself an acoustic design change.

[1]khardy@mtu.edu
[2]avcilett@mtu.edu
[3]pgodakaw@mtu.edu
[4]bnsharma@mtu.edu
[5]martha.c.brown@nasa.gov

1. INTRODUCTION

Modern turbofan engines produce increasingly broadband noise signatures, creating demand for acoustic liner technologies that attenuate sound over wide frequency ranges [1]. Additively manufactured porous metamaterials—particularly triply periodic minimal surface (TPMS) structures—offer high surface area for viscous dissipation within structurally robust, lightweight architectures. These materials have demonstrated strong broadband absorption in normal-incidence laboratory testing [2–5]. However, their performance under grazing flow conditions relevant to engine nacelles remains largely uncharacterized. A principal reason is that their interconnected pore networks are incompatible with standard impedance eduction methods—creating a situation in which the materials most likely to benefit from grazing-flow characterization are precisely those for which the standard characterization tools break down. Recent work on perforate-over-large-cell liners has similarly encountered eduction challenges arising from internal propagation [6].

This incompatibility raises two distinct engineering questions that the present work addresses. The first is a question of diagnostic compatibility: can standard locally-reacting eduction procedures be made to yield model-consistent impedances for these materials? The second is a question of design performance: what happens to the liner's attenuation characteristics when the intervention needed for eduction compatibility is applied? These are separate questions with potentially different answers, and the present study treats them as such.

The source of the diagnostic incompatibility is the distinction between locally-reacting and extended-reacting behavior. Standard grazing flow impedance eduction, as implemented in facilities such as NASA Langley's Grazing Flow Impedance Tube (GFIT), relies on the Ingard-Myers boundary condition [7–9]. This condition collapses the liner's internal response into a single surface impedance relation: a pointwise relationship between acoustic pressure and wall-normal particle velocity at the liner face. Impedance so defined is inherently a local quantity—it assumes that the liner's response at each surface location is independent of conditions elsewhere along the liner. This formulation makes the duct propagation problem tractable. Rather than modeling wave propagation within the liner volume, the entire liner response is represented by a single complex-valued impedance at the wall, reducing the problem to wave propagation in the duct alone [10–14]. The locality condition is satisfied when internal propagation is confined to the direction normal to the liner surface, as in traditional honeycomb-backed perforated liners where cell walls prevent streamwise communication within the core [1, 15–17]. TPMS structures can violate this locality condition under grazing-flow conditions. Their fully interconnected pore networks can permit streamwise propagation through the core, leading (under some conditions) to internal wave propagation along the liner's streamwise extent that the one-point surface impedance relation cannot represent. Standard eduction codes for locally-reacting liners can then produce educed impedances that are not suitable for bulk material characterization, with large, repeatable discontinuities at specific frequencies.

This paper investigates whether internal partitions (thin solid walls inserted at regular intervals along the liner's streamwise extent) can suppress internal streamwise propagation and produce a modified liner system for which the locally-reacting eduction framework yields consistent results. Throughout this paper, the following coordinate convention is adopted: *streamwise* refers to the direction of flow along the duct axis, *spanwise* refers to the direction across the duct width, and *through-thickness* (equivalently, *depth*) refers to the direction normal to the liner face (into the core depth). This convention is depicted in Figure 1a. Results are reported for six TPMS core geometries (gyroid, diamond, primitive, and three modified gyroids) tested across four partition spacings in no-flow and Mach 0.3 conditions. Beyond the eduction question, the effect of partitions on the liners' intrinsic acoustic response is examined. Blocking internal propagation paths changes the material itself, not only the measurement's consistency with the locally-reacting model.

2. EXPERIMENTAL METHODOLOGY

All tests were conducted in the GFIT, which generates grazing flows up to Mach 0.6 over acoustic liner samples installed in the upper wall of a rectangular duct with one soft (lined) wall. Flush-mounted microphones on the opposing wall measure the streamwise pressure field from 400 to 3000 Hz, and impedance is educed using the Prony method [18, 19]. Results in this study are presented up to 2700 Hz, as higher-order duct modes begin to cut on near this frequency and complicate the eduction process. The Prony method fits normal duct modes to the measured pressure field and substitutes the resulting axial propagation constants into the Ingard-Myers boundary condition to extract the normalized surface impedance at each frequency [7, 8]. In essence, the method solves an inverse problem: given the measured pressure field along the duct wall, it seeks the surface impedance that, when imposed as a boundary condition in the duct propagation model, best reproduces the observed data. The impedance is not measured directly but inferred from the spatial structure of the acoustic field in the duct [19]. A source plane level of 140 dB was maintained throughout testing to ensure adequate signal-to-noise ratio at higher Mach numbers. Linearity of the acoustic response was verified by comparing results at 120 dB and 140 dB source levels. No significant differences were observed, confirming that nonlinear effects associated with the pore geometry are not a concern at these source levels.

The system computes a correlation metric between the educed impedance's back-calculated pressure profile and the measured wall pressure data. This metric quantifies the degree to which the educed impedance, when used in the duct propagation model, reproduces the measured pressure field. A value of 100% indicates perfect agreement between measured and predicted wall pressures. High correlation is necessary evidence that the educed impedance is consistent with the locally-reacting model; however, it is not by itself sufficient to guarantee that the impedance is unique or physically correct, since multiple impedance values could in principle reproduce a given wall pressure distribution. In the present study, correlation values consistently above 85% are used as a practical threshold, informed by known locally-reacting liners tested in the GFIT [6, 20], to indicate that the locally-reacting model provides an adequate representation of the measured data. Well-characterized locally-reacting liners typically produce values above 90–95%; the 85% threshold thus represents a minimum standard of adequacy, with higher values indicating more robust model consistency. Discontinuities in the educed impedance—particularly abrupt jumps in resistance or reactance at specific frequencies—are the primary evidence that the locally-reacting model assumptions are not satisfied. Sharp drops in correlation to 40–60% at the same frequencies provide confirmation that the eduction process has failed to converge on a physically consistent impedance.

2.1. Sample Design

Samples were designed with 2″ square internal cores at a through-thickness depth of 2″, encased in a 0.25″ solid shell on all sides except for the face exposed to the acoustic field. The base gyroid, diamond, and primitive share a nominal unit cell pitch (periodic repeat length) of 0.2″ (5.08 mm), giving approximately 10 unit cells across the 2″ core depth; these three topologies differ substantially in pore connectivity and surface geometry despite sharing the same pitch. The elongated gyroids use the same base pitch, scaled by a $3\times$ stretch factor. The streamwise-elongated gyroid has a 0.6″ pitch in the streamwise direction and 0.2″ in the other two. The depth-elongated gyroid (i.e., elongated in the through-thickness direction) has a 0.6″ pitch in that direction and 0.2″ in-plane. The 45-degree case is a rotation of the depth-elongated geometry. Six TPMS configurations were tested: a base gyroid, a streamwise-elongated gyroid (3× stretch in the streamwise direction), a depth-elongated gyroid (3× stretch in the through-thickness direction), a 45-degree rotated depth-elongated gyroid, a diamond, and a primitive. Each unit cell is depicted in Figure 1(b)–(g). All cores were designed at 40% relative density. While relative density characterizes the solid fraction, it does not by itself determine the transport properties (permeability, hydraulic radius, tortuosity) that govern acoustic propagation and dissipation within the pore network; these properties vary with topology even at fixed relative density.

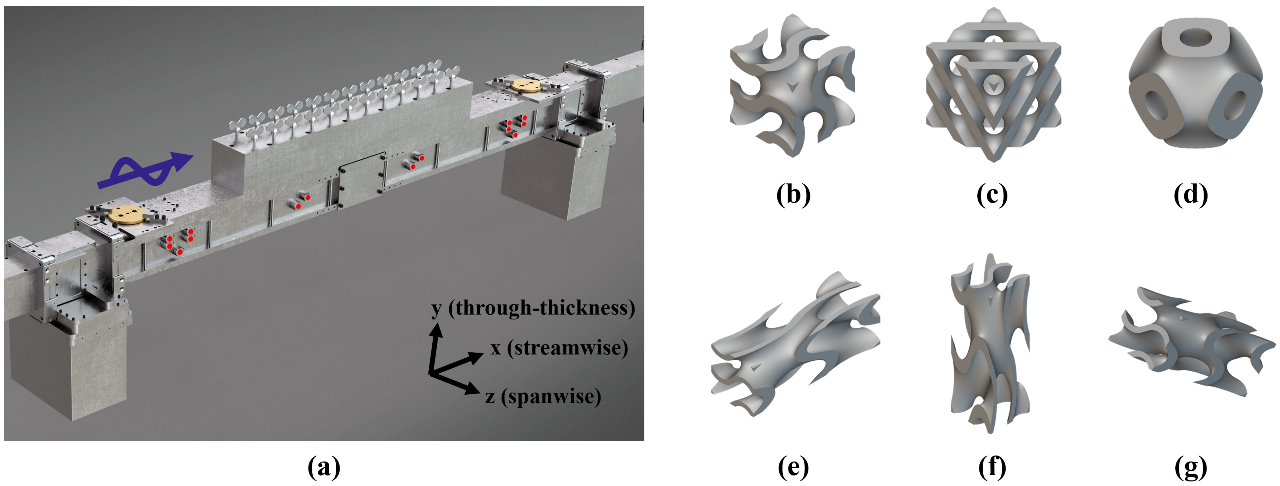

Figure 1: (a) A 3D rendering of GFIT with the coordinate convention used in this paper: x (streamwise), y (through-thickness), z (spanwise). The acoustic liner is installed into the top of the waveguide opposite the array of microphones on the lower wall. Panels (b)–(g) show unit cells for the (b) gyroid, (c) diamond, (d) primitive, (e) streamwise-elongated gyroid, (f) depth-elongated gyroid, and (g) 45-degree rotated depth-elongated gyroid

In all flow conditions, a 28 cgs Rayls wire mesh was adhered to the exposed face to reduce aerodynamic drag and self-noise generation. The mesh increases resistance across the frequency range; its interaction with the extended-reaction behavior of the core is discussed in Section 3.1.

2.2. Modular Snap-Fit Assembly

To enable systematic variation of partition spacing without reprinting entire samples, a modular snap-fit system was developed, pictured in Figure 2. The 20″ total core length was composed of individual blocks (1″ or 2″ lengths) joined by two types of clips: standard clips for seamless joints and specialized clips that hold a 0.05″ solid partition between adjacent blocks. Partitions are oriented normal to the streamwise direction, so that they physically interrupt any streamwise propagation paths within the core while preserving direct through-thickness access from the liner face to the backing wall. However, partitions also alter the through-thickness acoustic response by subdividing the communicating volume and modifying the local boundary conditions within each compartment. This system enabled testing of four partition configurations for each core geometry: no partitions, 4″ spacing, 2″ spacing, and 1″ spacing. A validation test comparing a gyroid assembled from 4″ blocks to one assembled from 1″ blocks in a non-partitioned, no-flow configuration confirmed that the snap-fit joints were acoustically transparent.

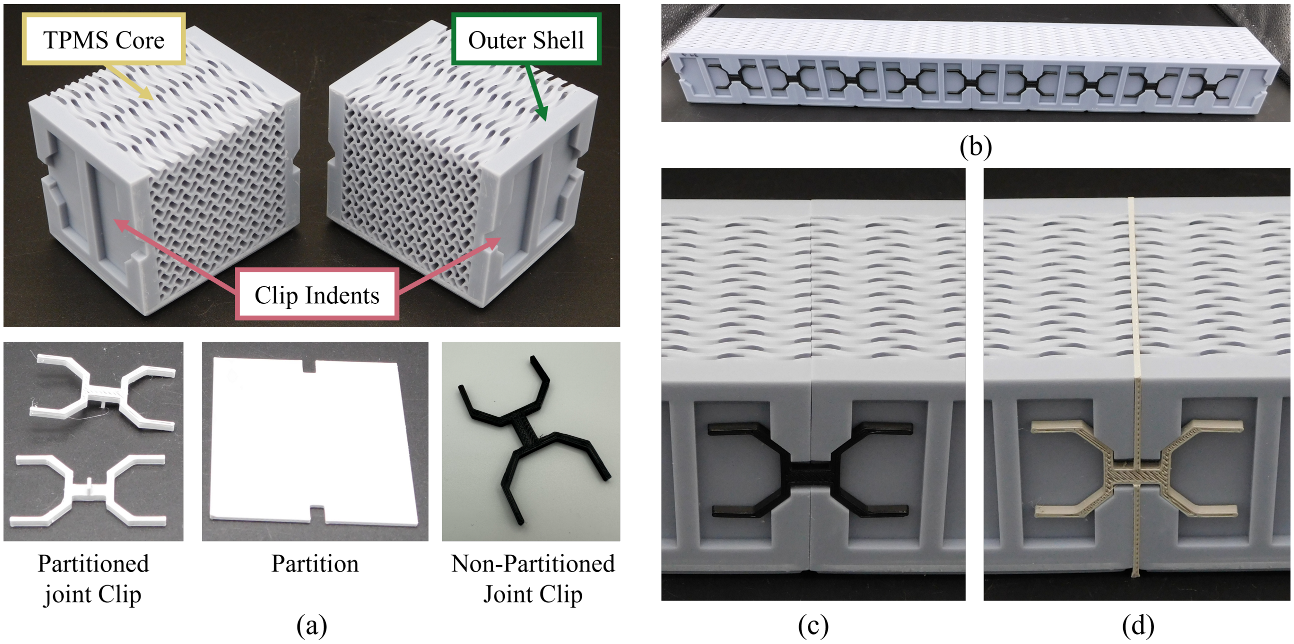

Figure 2: Snap-fit system. (a) All components of the snap-fit system, including 2″ blocks with TPMS core, outer shell, clip indents, clips, and partitions. (b) A fully assembled sample. (c) Close-up of a non-partitioned joint. (d) Close-up of a partitioned joint.

Samples were printed on an ELEGOO Saturn 4 MSLA resin printer in Grey Standard 1.0 resin at 50 µm layer thickness. Care was taken during mesh adhesion to eliminate bubbles and folds, which were found to produce measurable artifacts in the acoustic data.

3. RESULTS AND DISCUSSION

3.1. Eduction Discontinuities and the Effect of Partitions

Figure 3 establishes the baseline contrast between locally-reacting and extended-reacting behavior in the GFIT. For this comparison, a ceramic tubular liner (CT57) that has been well-characterized and established as locally-reacting by NASA Langley was tested [11, 12, 21]. Because the raw educed impedance and correlation spectra tend to be noisy, all spectra shown in this paper were processed using two passes of a five-point moving average filter. Reported correlation values and discontinuity frequencies are based on the processed spectra. The liner produces smooth resistance and reactance spectra characteristic of a locally-reacting sample [20]: the reactance follows a cotangent-like profile and the Prony correlation remains uniformly above 85%. The unpartitioned base gyroid, by contrast, exhibits an abrupt reactance transition near 1230 Hz accompanied by a resistance dip at the same frequency, and the Prony correlation drops to 37% at that frequency. This feature is repeatable across tests and indicates loss of consistency between the measured wall pressure field and the locally-reacting eduction model. Because the gyroid is a bulk porous material with interconnected porosity, locally-reacting impedance is not expected to fully characterize its acoustic behavior. The observation is consistent with internal streamwise propagation within the interconnected gyroid network, whose pore channels are continuous in all three spatial directions. Such behavior would produce departures from locally-reacting behavior that the Ingard-Myers boundary condition cannot represent.

The no-flow, no-mesh results show that partition effectiveness in producing locally-reacting

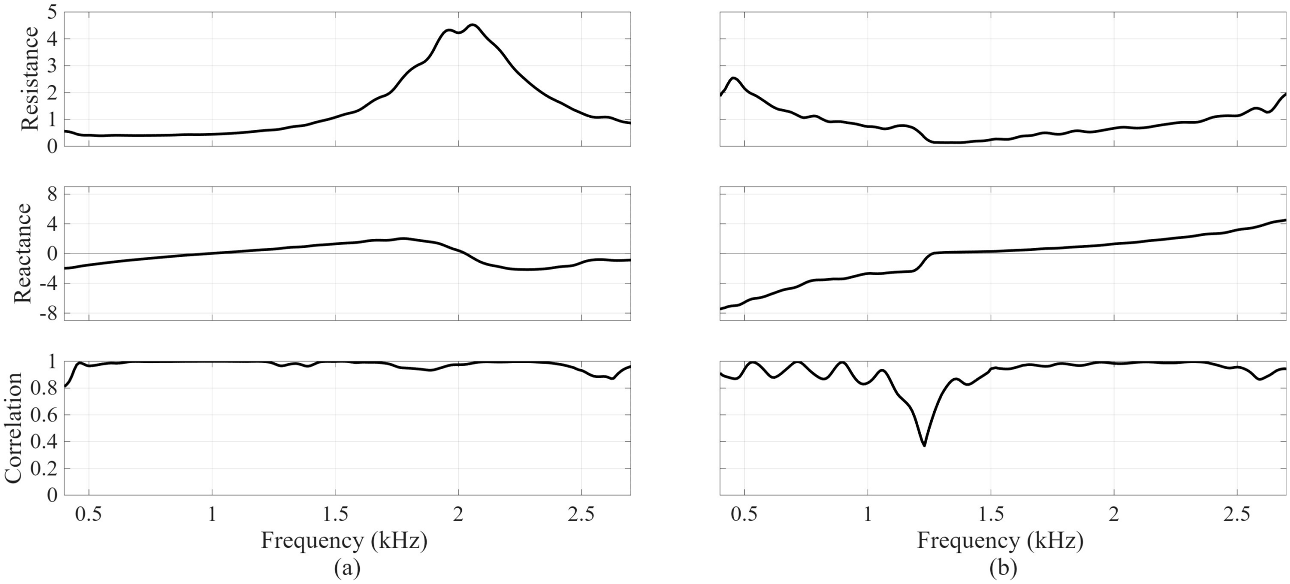

Figure 3: Impedance and Prony correlation under no-flow conditions comparing (a) the CT57 ceramic tubular calibration liner and (b) the unpartitioned Base Gyroid. The correlation dip near 1.2 kHz in the Base Gyroid coincides with the impedance discontinuity.

behavior depends strongly on core topology. For the base gyroid (Figure 4), the unpartitioned configuration shows a single dominant correlation dip to 37% at 1230 Hz, confirming that the impedance discontinuity seen in Figure 3 results in a loss of consistency with the locally-reacting eduction model. Throughout the remainder of this paper, correlation drops are used as confirmation of impedance discontinuities, with the understanding that correlation is an output of the eduction method and serves as an indicator of how well the locally-reacting model fits the measured data. With 4″ partitions, the impedance discontinuity shifts to lower frequency and its severity is reduced. With 2″ partitions, the discontinuity is eliminated and correlation remains above 90% across the measured band. The 1″ spacing produces results virtually identical to 2″, suggesting that 2″ spacing—which equals the through-thickness core depth—is sufficient to produce behavior consistent with the locally-reacting eduction framework for this geometry. The relationship between this threshold and the unit cell dimensions is discussed in Section 3.3.

The diamond and primitive geometries follow a similar pattern. Both show correlation drops in the unpartitioned case (to 49% for the diamond at 1220 Hz) that are progressively eliminated with decreasing partition spacing. However, not all geometries respond equally well. Figure 5 shows the depth-elongated, streamwise-elongated, and 45-degree cases. The depth-elongated and streamwise-elongated gyroids both show persistent, significant correlation dips even at 2″ spacing, with Prony correlation fluctuating around the 85% threshold (80–90% range) compared with consistently above 95% for the base gyroid. The 45-degree gyroid responds more readily to partitioning, similar to the base gyroid. These topology-dependent differences are discussed further in Section 3.3.

Under the realistic conditions (wire mesh, Mach 0.3) included in Figure 6, the unpartitioned correlation floors rise from approximately 40% to 60–70% for most geometries, even before partitions are added. This partial suppression of eduction artifacts under mesh and flow suggests that the added face treatment and grazing-flow condition interact with the extended-reaction behavior in a manner not fully explained by a simple uniform resistance addition. One possibility is that the mesh preferentially

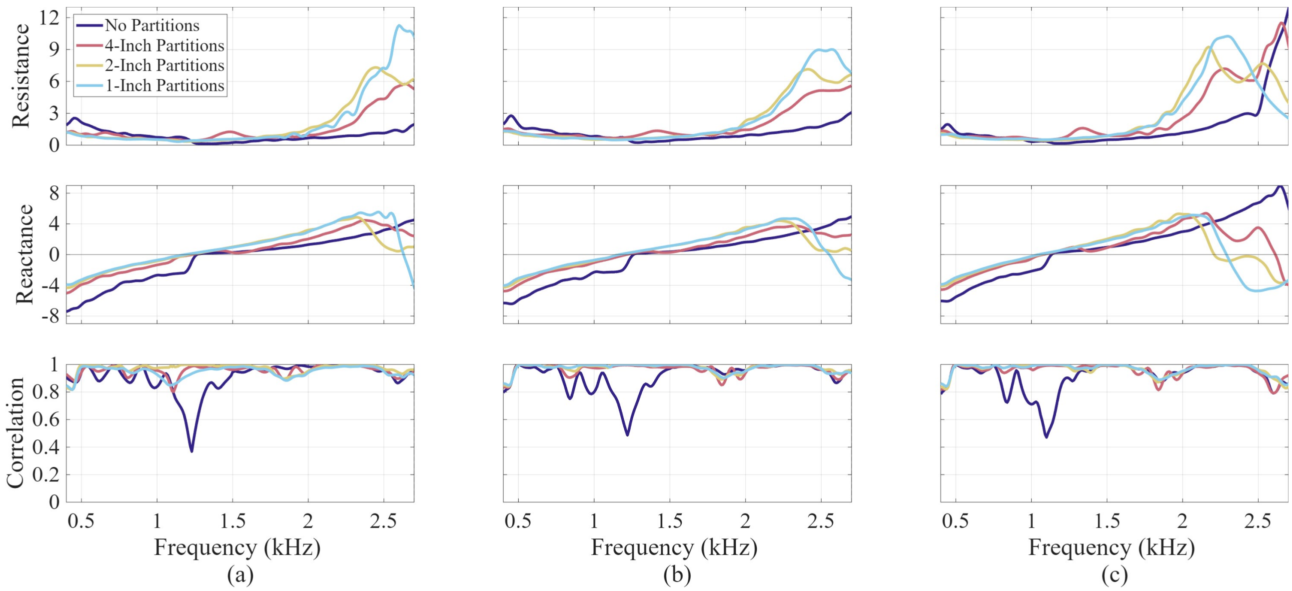

Figure 4: Effect of partitions on the (a) Base Gyroid, (b) Diamond, and (c) Primitive in no-flow and no-mesh conditions. All three geometries share the same 5.08 mm unit cell pitch; partition response differences reflect topology, not cell count.

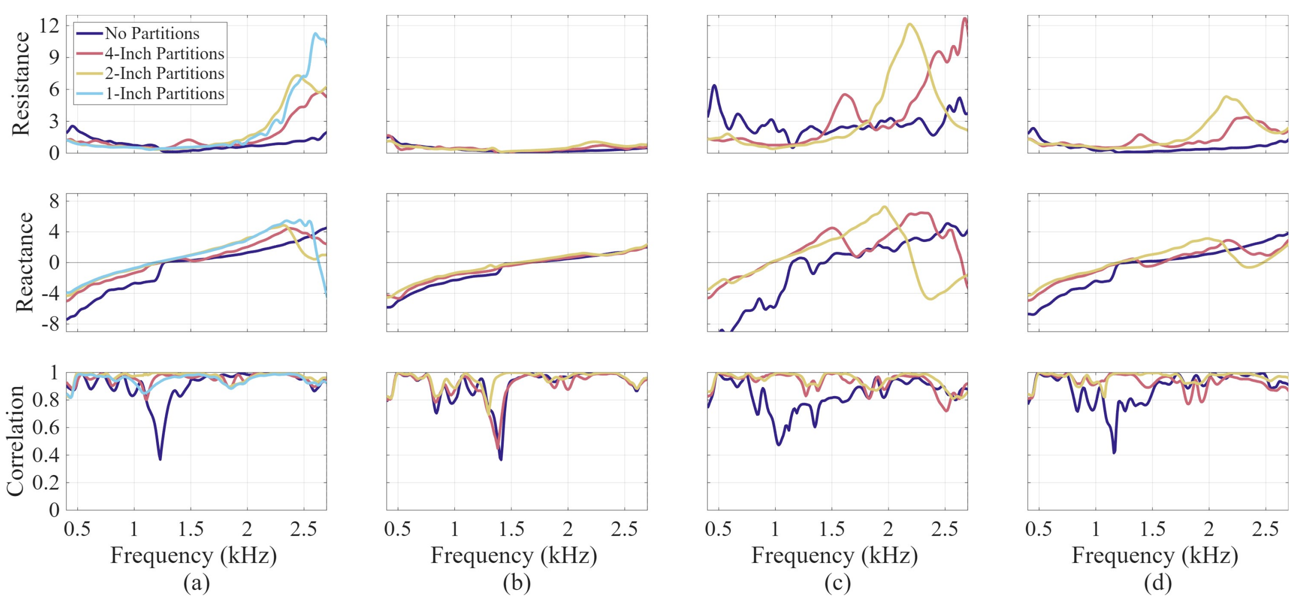

Figure 5: Effect of partitions on the (a) Base Gyroid, (b) Depth-Elongated, (c) Streamwise-Elongated, and (d) 45-Degree in no-flow and no-mesh conditions. Note the systematic shift of the discontinuity frequency with partition spacing in the Base Gyroid and 45-Degree cases.

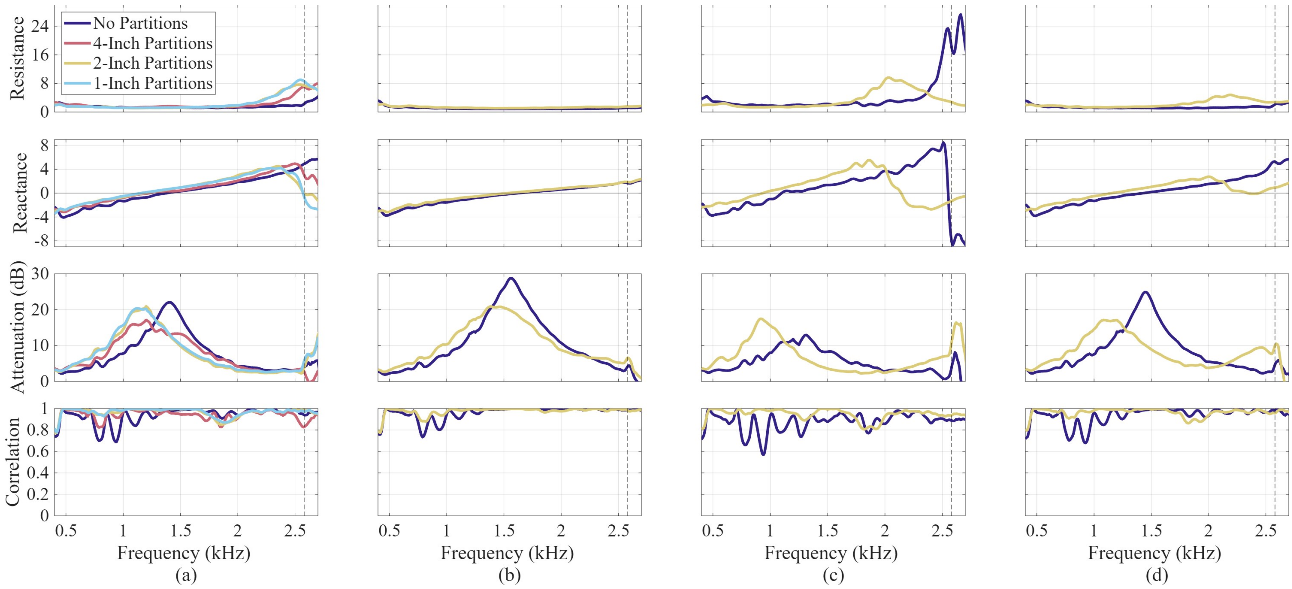

Figure 6: Effect of partitions on the (a) Base Gyroid, (b) Depth-Elongated, (c) Streamwise-Elongated, and (d) 45-Degree with wire mesh and flow at Mach 0.3. Higher-order modes cut on near 2.7 kHz, and therefore data beyond this frequency are not shown.

suppresses streamwise communication at the liner surface relative to through-thickness propagation—a point that warrants further investigation. The addition of 2″ partitions under these conditions brings most geometries above approximately 95% correlation for the majority of the frequency range, though the streamwise-elongated gyroid retains more residual correlation fluctuation than the others.

3.2. Partitions Alter Acoustic Behavior

A central finding of this study is that partitions do not merely improve the consistency of impedance eduction with the locally-reacting model—they change the acoustic behavior of the liner itself. The partitioned liner is a different acoustic system from the unpartitioned liner, and the educed impedance characterizes this modified system. Figure 6 shows no-partition and 2″ partition configurations alongside intermediate spacings under mesh and Mach 0.3 conditions; the following discussion focuses on the contrast between the unpartitioned and 2″ cases.

For most geometries, three consistent effects are observed. First, partitions increase the acoustic resistance, particularly at higher frequencies under no-flow and no-mesh conditions. Second, the reactance zero-crossing—which is often associated with the frequency of near-maximum attenuation—shifts to lower frequencies, consistent with a change in the effective inertive-compliant balance of the subdivided core [22]. These two effects may be coupled: the downward shift in resonance also moves the antiresonance structure, which could account for part of the apparent resistance increase at higher frequencies. The specific mechanism of this shift is not isolated by the present data; plausible contributing factors include altered effective cavity volume per connected pathway, modified tortuosity, changed viscous and thermal boundary-layer participation in the subdivided geometry, and altered communication between subvolumes. Third, peak attenuation magnitude decreases: for the depth-elongated gyroid, peak attenuation drops from 29 dB to 21 dB; for the 45-degree gyroid, from 25 dB to 17 dB.

This reduction in peak attenuation is partially offset by a broadening of the attenuation bandwidth for some geometries. The base gyroid, depth-elongated, and 45-degree cases all show visibly broader attenuation curves with partitions. The streamwise-elongated gyroid is a notable exception: its unpartitioned response already exhibits relatively low, broad attenuation (peak 13 dB) along with anomalous high-frequency resistance and reactance behavior. Partitions regularize this response without substantially changing the peak attenuation level.

It is important to note that improved eduction consistency and altered acoustic behavior may not share the same cause. Partitions simultaneously interrupt streamwise connectivity (a topological change) and introduce additional solid surface area with associated viscous and thermal dissipation (a loss change). Either effect alone could improve Prony correlation: the first by suppressing the streamwise connectivity responsible for the extended-reacting behavior, the second by damping internal propagation until it no longer significantly affects the wall pressure field. The present data do not separate these two contributions.

For liner design, the implication is that partitions should be treated as a design variable, one that trades eduction compatibility against modifications to the impedance and attenuation profile.

3.3. Geometry-Dependent Response

As shown in Section 3.1, partition effectiveness in producing locally-reacting behavior varied substantially across core topologies, from fully resolved at 2″ spacing for the base gyroid to persistently resistant for the depth-elongated and streamwise-elongated gyroids.

The simplest geometric explanation for this ordering would be that partition sensitivity scales with the number of unit cells per partition interval—that is, geometries with larger streamwise pitch require more partitions to interrupt a given length. The data do not support this. The base gyroid, diamond, primitive, and depth-elongated gyroid all share the same 0.2″ streamwise pitch (approximately 10 cells per 2″ partition interval), yet span the full range of partition sensitivity observed in this study—from fully resolved at 2″ spacing to persistently resistant. This shows that streamwise unit cell count alone is not a sufficient predictor and points instead to topology-dependent connectivity or related transport structure.

The elongated gyroids sharpen this conclusion. The streamwise-elongated gyroid has a 0.6″ streamwise pitch (approximately 3.3 cells per 2″ partition interval), while the depth-elongated has a 0.2″ streamwise pitch (identical to the base gyroid) but 0.6″ in the through-thickness direction. If streamwise pitch governed partition sensitivity, the streamwise-elongated should be the most resistant geometry. Instead, both elongated variants show comparable levels of residual correlation fluctuation with 2″ partitions in no-flow conditions (Figure 5), though the streamwise-elongated retains slightly more fluctuation under flow (Figure 6). The depth-elongated is among the most resistant despite having the same streamwise pitch as the readily partitioned base gyroid, which suggests that the relevant parameter involves the topology of internal connectivity—which is altered by the through-thickness stretch in ways not captured by pitch alone.

Having eliminated pitch as a sufficient predictor, the ordering appears better described by the degree of streamwise connectivity—used here as a qualitative descriptor of how readily the pore network supports continuous propagation paths in the streamwise direction. The depth-elongated gyroid, despite being stretched in the through-thickness direction, still appears to support internal propagation patterns that are more resistant to interruption by streamwise partitions; the streamwise-elongated gyroid exhibits comparable behavior. The base gyroid's pore network, while fully interconnected, does not appear to exhibit obvious preferential streamwise channels, making it more amenable to disruption by transverse partitions. A quantitative metric—such as a directional percolation measure, geodesic tortuosity along the streamwise axis, or a connected-path persistence length—would be needed to place the geometry-dependent response on a predictive footing. Developing such a metric is a target for future computational work.

The observation that the effective partition threshold (2″) equals the through-thickness core depth for the readily partitioned geometries also warrants note. For the 5.08 mm-pitch TPMS geometries, the 2″ threshold corresponds to approximately 10 unit cells in the streamwise direction, while even the finest tested spacing of 1″ still spans roughly 5 unit cells. The threshold is therefore not at the single-unit-cell scale but at a mesoscale that may reflect a characteristic propagation or coherence length within the network. Whether the relevant scale is the through-thickness depth itself, a topology-dependent connectivity length, or some combination cannot be determined from the present data alone. Notably, Brown et al. [6] observed that a similar 2″ cross-sectional dimension produced locally-reacting behavior in perforate-over-air-cavity configurations, suggesting that this length scale may be related to the duct geometry as much as to the TPMS topology.

4. CONCLUSIONS

Internal partitions provide a practical strategy for producing modified porous liners that are substantially more compatible with standard grazing-flow impedance eduction. For geometries that responded readily to partitioning (base gyroid, diamond, primitive, 45-degree), 2″ partition spacing—equal to the through-thickness core depth—was sufficient to remove visible impedance discontinuities and increase Prony correlation above 90%. Geometries whose topology appears to support more persistent streamwise connectivity (depth-elongated and streamwise-elongated gyroids) were not fully regularized at 2″ spacing and retained residual artifacts even at the finest tested spacing, particularly under no-flow conditions. This suggests that partition effectiveness depends on the core's internal connectivity rather than a universal spacing threshold.

Partitions are not acoustically transparent. They increase resistance, shift resonance to lower frequencies, and reduce peak attenuation while broadening bandwidth for most topologies. The partitioned liner constitutes a distinct acoustic system, and the educed impedance characterizes this modified system rather than the original unpartitioned core. Improved Prony correlation indicates that the partitioned system is more consistent with the locally-reacting eduction framework; however, because impedance eduction is an inverse problem, high correlation alone does not guarantee that the educed impedance is unique or that it represents the true surface impedance of the partitioned liner.

For practical liner design, partitions should be incorporated as a co-designed structural feature that simultaneously promotes behavior more consistent with a locally-reacting treatment and shapes the impedance profile. The present results do not fully separate the contributions of topological interruption (blocking streamwise propagation paths) from additional dissipation (added partition surface area), and resolving this decomposition would clarify the physical basis of the partition effect.

The modular snap-fit assembly proved reliable for systematic parametric testing and may be useful for other multi-configuration experimental campaigns. Future work will focus on computational analysis of the internal propagation structure to identify the mechanisms driving the eduction discontinuities, development of a quantitative streamwise connectivity metric for predictive partition design, and exploration of bulk acoustic property extraction as an alternative to locally-reacting impedance eduction for materials that remain extended-reacting.

5. ACKNOWLEDGEMENTS

The authors thank Alonso “Max” Reid for his assistance with testing and sample assembly, and Chris Shoemaker and Brian Howerton for their contributions to testing and data processing. This work was supported by a NASA Space Technology Graduate Research Opportunity.

REFERENCES

[1] Tamer Elnady and Hans Boden. On Semi-Empirical Liner Impedance Modeling with Grazing Flow. In *9th AIAA/CEAS Aeroacoustics Conference and Exhibit*, Hilton Head, South Carolina, May 2003. American Institute of Aeronautics and Astronautics.

[2] Janith Godakawela, Amulya Lomte, and Bhisham Sharma. Sound absorption in uniform and layered gyroid and diamond triply periodic minimal surface porous absorbers. *Applied Acoustics*, 236:110761, 2025.

[3] Junxiang Fan, Bo Song, Lei Zhang, Xiaobo Wang, Zhi Zhang, Shuaishuai Wei, Xiao Xiang, Xuefeng Zhu, and Yusheng Shi. Structural design and additive manufacturing of multifunctional metamaterials with low-frequency sound absorption and load-bearing performances. *International Journal of Mechanical Sciences*, 238:107848, January 2023.

[4] Xinwei Li, Jun Wei Chua, Xiang Yu, Zhendong Li, Miao Zhao, Zhonggang Wang, and Wei Zhai. 3D-Printed Lattice Structures for Sound Absorption: Current Progress, Mechanisms and Models, Structural-Property Relationships, and Future Outlook. *Advanced Science*, 11(4):2305232, January 2024.

[5] Jun Wei Chua, Xinwei Li, and Wei Zhai. Design, multiscale modelling, and experimental characterisation of TPMS-based composite lattices with enhanced sound absorption. *Composite Structures*, 370:119437, October 2025.

[6] Martha C. Brown, Chelsea Dodge, Jordan R. Kreitzman, and Michael G. Jones. Assessment of Acoustic Behavior for Perforate-Over-Large-Cell Liners. In *AIAA AVIATION 2023 Forum*, 2023.

[7] Uno Ingard. Influence of Fluid Motion Past a Plane Boundary on Sound Reflection, Absorption, and Transmission. *The Journal of the Acoustical Society of America*, 31(7):1035–1036, July 1959.

[8] M.K. Myers. On the acoustic boundary condition in the presence of flow. *Journal of Sound and Vibration*, 71(3):429–434, August 1980.

[9] Andre Spillere, Julio Cordioli, and Hans Bodén. On the Effect of Boundary Conditions on Impedance Eduction Results. In *23rd AIAA/CEAS Aeroacoustics Conference*. American Institute of Aeronautics and Astronautics, June 2017.

[10] Brian M. Howerton, Michael G. Jones, and Douglas M. Nark. An Improved Impedance Eduction Process for the NASA Langley GFIT. In *AIAA AVIATION 2020 FORUM*, Virtual Event, June 2020. American Institute of Aeronautics and Astronautics.

[11] Michael Jones, Willie Watson, and Douglas Nark. Effects of Flow Profile on Educed Acoustic Liner Impedance. In *16th AIAA/CEAS Aeroacoustics Conference*, Stockholm, Sweden, June 2010. American Institute of Aeronautics and Astronautics.

[12] Willie R. Watson and Michael G. Jones. A Comparative Study of Four Impedance Eduction Methodologies Using Several Test Liners. In *19th AIAA/CEAS Aeroacoustics Conference*, Berlin, Germany, May 2013. American Institute of Aeronautics and Astronautics.

[13] Xiwen Dai and Yves Aurégan. Acoustic of a perforated liner with grazing flow: Floquet-Bloch periodical approach versus impedance continuous approach. *The Journal of the Acoustical Society of America*, 140(3):2047–2055, September 2016.

[14] Ygaäl Renou and Yves Aurégan. Failure of the Ingard–Myers boundary condition for a lined duct: An experimental investigation. *The Journal of the Acoustical Society of America*, 130(1):52–60, July 2011.

[15] Michael G. Jones and Willie R. Watson. Effects of Liner Length and Attenuation on NASA Langley Impedance Eduction. In *22nd AIAA/CEAS Aeroacoustics Conference*, Lyon, France, May 2016. American Institute of Aeronautics and Astronautics.

[16] Martha Brown, Michael Jones, and Willie Watson. Uncertainty Analysis of the Grazing Flow Impedance Tube. In *18th AIAA/CEAS Aeroacoustics Conference*, Colorado Springs, CO, June 2012. American Institute of Aeronautics and Astronautics.

[17] R. J. Astley and A. Cummings. A finite element scheme for attenuation in ducts lined with porous material: Comparison with experiment. *Journal of Sound and Vibration*, 116(2):239–263, July 1987.

[18] Willie R. Watson, Mark H. Carpenter, and Michael G. Jones. Performance of Kumaresan and Tufts Algorithm in Liner Impedance Eduction with Flow. *AIAA Journal*, 53(4):1091–1102, April 2015.

[19] R. Kumaresan and D. Tufts. Estimating the parameters of exponentially damped sinusoids and pole-zero modeling in noise. *IEEE Transactions on Acoustics, Speech, and Signal Processing*, 30(6):833–840, December 1982.

[20] Michael Jones, Willie Watson, Maureen Tracy, and Tony Parrott. Comparison of two acoustic waveguide methods for determining liner impedance. In *7th AIAA/CEAS Aeroacoustics Conference and Exhibit*, Maastricht, Netherlands, May 2001. American Institute of Aeronautics and Astronautics.

[21] Brian M. Howerton, Havard Vold, and Michael G. Jones. Application of Swept Sine Excitation for Acoustic Impedance Eduction. In *25th AIAA/CEAS Aeroacoustics Conference*, Delft, The Netherlands, May 2019. American Institute of Aeronautics and Astronautics.

[22] T. Parrott and H. Lester. Calculated and measured performance of a 'near ideal' locally reacting duct liner in grazing incidence. In *6th Aeroacoustics Conference*, Hartford, CT, June 1980. American Institute of Aeronautics and Astronautics.